

Simultaneous Measurement of Thermal Diffusivity, Thermal Conductivity and Specific Heat by Impulse-Response Photopyroelectric Spectrometry

Application to the Superconductor $\text{YBa}_2\text{Cu}_3\text{O}_{7-x}$

S. B. Peralta, Z. H. Chen, and A. Mandelis

Photoacoustic and Photothermal Sciences Laboratory, Department of Mechanical Engineering, and Ontario Laser and Lightwave Research Centre, University of Toronto, Toronto, Ontario M5S 1A4, Canada

Received 5 November 1990/Accepted 16 January 1991

Abstract. A novel photothermal technique is developed, which enables the simultaneous measurement of the thermal diffusivity α , thermal conductivity κ , and the specific heat C of a sample. The technique is based on frequency-modulated time-delay photopyroelectric spectrometry (FM-TDPS), which consists of chirped laser excitation of the sample and detection of the thermal impulse response by a thin-film pyroelectric detector. No calibration is required for the measurements; absolute values for α , κ , and C may be obtained without having to employ a reference sample. Results on superconducting $\text{YBa}_2\text{Cu}_3\text{O}_{7-x}$ are reported for the temperature range 50–300 K; the values obtained compare favorably with reported measurements of α , κ , and C for $\text{YBa}_2\text{Cu}_3\text{O}_{7-x}$, which previously required separate experiments for their determination.

PACS: 78.20 Hp, 74.30 Ek

The detection of radiation-induced thermal wave phenomena through the use of pyroelectric detectors, known as photopyroelectric spectrometry, has recently been demonstrated to be a simple and sensitive technique for the thermal analysis of condensed matter [1–4]. Photothermal techniques, of which photopyroelectric methods form a subset, have been widely applied in the measurement of such thermal parameters as the thermal diffusivity for liquids and solids, as well as in the characterization of the behavior of these thermal parameters at phase transitions. Among the various photothermal detection schemes, however, photopyroelectric methods combine extreme sensitivity with high temporal resolution, as well as low cost [5]; consequently photopyroelectric sensors based on such materials as polyvinylidene fluoride (PVDF) show great potential for use in various applications in thermal and spectroscopic work.

Most photopyroelectric experiments result in the measurement of either the thermal diffusivity or effusivity of a sample. In this paper we describe a method, based on photopyroelectric detection of the sample response to chirped laser excitation, which allows the simultaneous measurement of the thermal diffusivity α , thermal conductivity κ , and specific heat C of a sample. The technique requires no calibration, and absolute values for these thermal parameters may be obtained without preliminary measurements on a reference sample. As an example, we have applied the technique to the measurement of these thermal parameters through the superconducting tran-

sition of the high-temperature superconductor $\text{YBa}_2\text{Cu}_3\text{O}_{7-x}$ (YBCO).

The thermal properties of YBCO and the other oxide superconductors provide much invaluable information concerning the nature and mechanism of the superconductivity in these systems. In particular, work has concentrated on measurement of the specific heat [6–9] and the thermal conductivity [10–12] of these materials. Recently, photoacoustic and photothermal methods have been used in investigation of the thermal diffusivity α or thermal effusivity e of YBCO [13–15]; these quantities are functionally dependent on κ and C through the relations $\alpha = \kappa/\rho C$ and $e = (\kappa\rho C)^{1/2}$, where ρ is the density of the material. Further work on the determination of multiple thermal parameters of condensed phases from frequency-domain photoacoustic and photothermal signals has been reported using combinations of amplitude and phase channels [16–18]. In previous papers we reported the application of frequency-modulated time-delay photopyroelectric spectrometry (FM-TDPS) to the study of the thermal properties of the oxide superconductors. Specifically, we obtained the qualitative temperature profile of the thermal conductivity for YBCO [19], as well as quantitative measurements of the temperature dependence of the thermal diffusivity for YBCO and $\text{Bi}_2\text{Sr}_2\text{CaCu}_2\text{O}_x$ (BSCCO) [20–22].

Although the techniques mentioned above have been shown to give reasonable values for the simultaneous measurement of multiple thermal parameters, they have

several disadvantages: Most “classical” photothermal techniques only measure either the thermal diffusivity or effusivity, and require an independent measurement of the thermal conductivity to yield the specific heat; a variation of the frequency-domain technique [16–18] does yield a measurement of α , κ , and C , but requires a separate experiment on a reference sample for the purposes of normalization and calibration. In contrast, the impulse response (time-domain) technique presented here requires no preliminary normalization to provide simultaneous measurements of the above thermal parameters. In the present FM-TDPS measurements the sample is heated by a chirp-modulated cw laser, and the associated thermal response detected at the back surface by a fast risetime thin-film pyroelectric detector. The sample thermal impulse response is calculated from the input and output waveforms through cross correlation and fast Fourier transform (FFT) techniques [23–25], and α , κ , and C are obtained from the impulse response. The results are similar to those obtained with the frequency-domain method [26–27] except for the advantages we have noted above. For YBCO over the temperature range 50–300 K, α , κ , and C thus measured compare favorably with reported values, confirming the reliability of our technique.

1. Theoretical Background

1.1 Chirped Excitation

FM-TDPS involves a chirped excitation technique [25], in which a cw laser is modulated by a fast frequency sweep waveform $x(t)$, or chirp, before being focussed onto the sample. It has been previously noted [19–22] that chirped excitation has several advantages over laser flash methods, which have been the usual method for determining the thermal diffusivity of metals and oxides [13]. Chirped excitation is characterized by the low incident power density and high source stability inherent in cw laser systems. Consequently, the technique has the advantage of being able to work with samples having low optical damage thresholds; in addition, recent studies on the optical properties of high- T_c materials [29] have pointed to a switching from the superconducting to the normal state on irradiation with fast, high-power laser pulses. Chirped modulation also retains an advantage over single modulation frequency/lock-in techniques in that measurements are directly interpretable in terms of thermal pulse propagation times through the material.

If the power spectrum $G_{xx}(f)$ of the chirp is relatively flat across its frequency span, chirped excitation is equivalent, in the frequency domain, to pulsed excitation. As a consequence, chirped excitation enables one to obtain the impulse response of a material without actually using pulsed excitation. This may be shown as follows. If $y(t)$ is the instantaneous response of the sample to the exciting chirp, then the input power spectrum $G_{xx}(f)$ and the cross spectrum $G_{xy}(f)$ are given by

$$G_{xx}(f) = F[x(t)] \times F[x(t)]^*, \quad (1a)$$

$$G_{xy}(f) = F[x(t)] \times F[y(t)]^*, \quad (1b)$$

where F and F^* represent the Fourier transform and its complex conjugate, respectively. The impulse response is then obtained from the relation

$$h(\tau) = F^{-1}[G_{xy}(f)/G_{xx}(f)], \quad (2)$$

where τ is the time-delay domain variable. The experimental procedure then consists of obtaining the impulse response $I(t) = h(\tau)$ from a measurement of the input and output waveforms $x(t)$ and $y(t)$.

1.2 Pyroelectric Detection

Consider a sample of thickness l , affixed by its back surface to a pyroelectric detector with thickness d , pyroelectric coefficient p and dielectric constant ϵ . The current impulse response of the detector due to heat flow through the sample may be obtained through a Green’s function treatment [25], yielding

$$I(t) = \frac{pdA}{\epsilon t^{3/2}} \sum_{n=0}^{\infty} (-1)^n \beta_{32}^n [\tau_{1n}^{1/2} e^{-\tau_{1n}/4t} - 2\tau_{2n}^{1/2} e^{-\tau_{2n}/4t} + \tau_{3n}^{1/2} e^{-\tau_{3n}/4t}]. \quad (3)$$

The thermal coupling coefficients between adjacent layers i and j in the air-sample-detector-backing system – labelled 1 to 4, respectively – are given by $\beta_{ij} = (b_{ij} - 1)/(b_{ij} + 1)$, where $b_{ij} = \kappa_i \alpha_j^{1/2} / \kappa_j \alpha_i^{1/2}$. Here κ_n and α_n are the thermal conductivities and diffusivities of the n th layer. The following definitions have been made:

$$\tau_{1n}^{1/2} = \frac{2nd}{\alpha_3^{1/2}} + \frac{l}{\alpha_2^{1/2}}, \quad (4a)$$

$$\tau_{2n}^{1/2} = \frac{(2n+1)d}{\alpha_3^{1/2}} + \frac{l}{\alpha_2^{1/2}}, \quad (4b)$$

$$\tau_{3n}^{1/2} = \frac{2(n+1)d}{\alpha_3^{1/2}} + \frac{l}{\alpha_2^{1/2}}, \quad (4c)$$

and A is a constant incorporating the static thermal properties of the sample-pyroelectric system:

$$A = - \frac{(\alpha_3 \alpha_2)^{1/2}}{2\sqrt{\pi} \alpha_2 (b_{32} + 1)}. \quad (5)$$

Three approximations were made in deriving (3): a large thermal mismatch at the sample front surface ($b_{12} \ll 1$ or $\beta_{12} \cong -1$); the use of a metal backing for the thin-film pyroelectric detector ($b_{43} \gg 1$ or $\beta_{43} \cong 1$); and a sample that is thermally thick compared to the detector ($\tau_2 \gg \tau_3$, where τ_n is the time for a unit heat impulse to travel through the n th layer; equivalently, $l^2/\alpha_2 \gg d^2/\alpha_3$). All these approximations are valid for the arrangement used in our experiment.

Equation (3) defines a pulse which rises to a peak value, and then declines to a slightly negative value before gradually rising again to zero at very long times. Along with the dependence on the sample thermal parameters, the shapes of the responses are sensitive to the detector properties; for a PVDF detector, as in our case, $\alpha_3 = 8 \times 10^{-8} \text{ m}^2/\text{s}$ and $\kappa_3 = 0.19 \text{ W/m} \cdot \text{K}$ for the detector

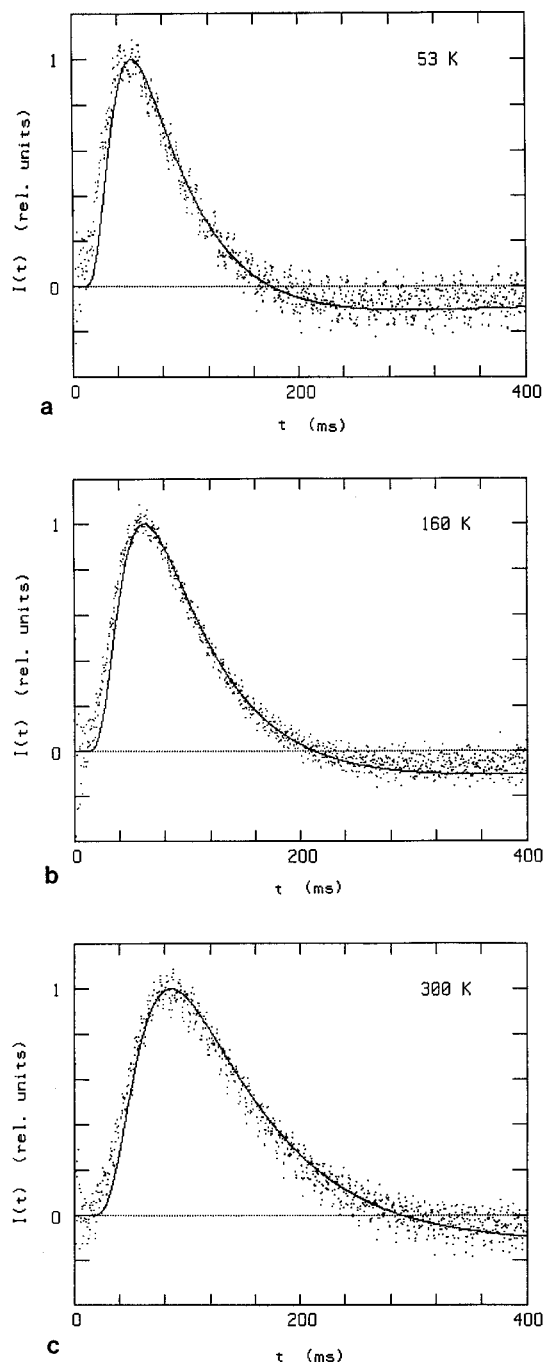


Fig. 1a–c. Representative experimental photopyroelectric responses for $\text{YBa}_2\text{Cu}_3\text{O}_{7-x}$ (YBCO) at **a** 53 K, **b** 160 K, and **c** 300 K. Similar responses were taken at different temperatures. Solid curves correspond to the theoretical $I(t)$ using **a** $\alpha = 1.486 \times 10^{-6} \text{ m}^2/\text{s}$ and $\kappa = 3.674 \text{ W/m}\cdot\text{K}$, **b** $\alpha = 1.268 \times 10^{-6} \text{ m}^2/\text{s}$ and $\kappa = 4.422 \text{ W/m}\cdot\text{K}$, and **c** $\alpha = 9.22 \times 10^{-7} \text{ m}^2/\text{s}$ and $\kappa = 4.734 \text{ W/m}\cdot\text{K}$. The chirped excitation bandwidth was 1 kHz

thermal diffusivity and conductivity, respectively [25]. An example of the theoretical pulse shape is shown by the solid curves in Fig. 1a–c.

Two characteristic times in the pyroelectric current response are important to our discussion: the zero-crossing point τ_0 , at which

$$[I(t)]_{t=\tau_0} = 0 \quad (6)$$

and the peak time τ_p at which the response reaches a maximum. It can be shown [19] that τ_p is linear with l^2/α , where we have written $\alpha = \alpha_2$, with a slope $F_p = 0.08$ for PVDF detection, independent of $\kappa = \kappa_3$; this is a consequence of the fact that the current response at earlier times is a strong function of the thermal diffusivity, and is only very weakly dependent on the sample thermal conductivity. F_p is only dependent on the thermal and geometric properties of the detector. Thus, by monitoring the time at which the impulse response reaches its maximum, the sample thermal diffusivity can be calculated from the equation

$$\alpha = F_p \left(\frac{l^2}{\tau_p} \right). \quad (7)$$

Using this value for α in (6), one then obtains a value for the sample thermal conductivity κ . The specific heat may then be easily calculated from the relation

$$C = \frac{\kappa}{\rho\alpha}. \quad (8)$$

Experimentally, the amplitude of the impulse response defined by (3) is normalized to the peak value. Since this normalization affects neither τ_p nor $I(\tau_0) = 0$, no calibration of the system is required to obtain relative values for α , κ , and C . In the case of the frequency-domain technique [26, 27] an extra calibration step using a reference sample is required because the thermal parameters obtained are extremely sensitive to the absolute values of the measured quantities – the amplitude and phase of the photothermal signal.

2. Experimental Arrangement

A standard photopyroelectric arrangement was used in the present work. The pyroelectric impulse responses were excited with 20 mW incident power from the 488 nm line of an Ar^+ laser. The cw beam was chirped by an acousto-optic modulator, driven by a waveform synthesizer, before being focussed onto the sample front surface. The driving chirp waveform $x(t)$ had an amplitude of 85 mV, and a flat power spectrum over the modulation bandwidth of 1 kHz, so that the resulting chirped cw laser beam satisfied the criterion for mathematical equivalence to pulsed excitation.

The ceramic YBCO samples were prepared by standard solid state reaction of Y_2O_3 , BaCO_3 , and CuO powders, mixed and calcined at 900–950°C for 10 h. Sintering was carried out at 950°C for a further 10 h, and then cooling, at a rate of about 100°C/h, with an intermediate holding at 500°C for 5 h. The pellets were roughly $3 \times 3 \times 1 \text{ mm}^3$ in size, and the superconducting transition was $T_c = 78 \text{ K}$ for the sample in the measurements reported [31].

The detector consisted of a 28 μm -thick film of PVDF, much thinner than the sample, surface-metallized with nickel electrodes and supported on a stainless steel backing. The YBCO samples were fixed to the detector by means of a thin thermal compound layer, whose contri-

bution to the PPE signal above 50 K is negligible [19, 32]. The sample and detector were housed in a cryogenic system with optical access through a vacuum-sealed quartz window. The experimental temperature range was 50–300 K, monitored by a gold/iron-constantan thermocouple mounted at the end of the copper cold finger to which the sample/detector holder was also attached. The detector output was fed to a fast current amplifier before being directed to the $y(t)$ system input of an FFT analyzer. The current impulse response was then recovered by correlation and FFT operations on $x(t)$ and $y(t)$ as discussed above.

3. Results and Discussion

The capability of the described photopyroelectric technique to monitor simultaneously the temperature dependence of α , κ , and C was tested over the high- T_c superconducting transition of YBCO. Figure 1a–c shows representative impulse responses for the YBCO sample at 53, 160, and 300 K, normalized at $I(\tau_p)$. Qualitatively, the impulse response at varying temperatures is the same, except for a narrowing of the pulse at lower temperatures, due to the variation in YBCO thermal parameters. The spike in the experimental impulse response at early times ($< 50 \mu\text{s}$) is due to the detector response to light leakage onto the surface of the film. The initial PVDF spike is negligible in our analysis, since the fastest thermal transit time through our sample is on the order of tens of milliseconds. The solid curves are the theoretical impulse response calculated from (3), using values for α and κ obtained as discussed above, from (6, 7). The fit of the theoretical expression to the experimentally obtained data is excellent, especially within the region from τ_p to τ_0 .

Figure 2 shows the behavior of the time delay variables τ_p and τ_0 in the temperature range 50–300 K, clearly exhibiting a proportional increase with temperature due to the broadening of the impulse response. Because of the diffusive nature of thermal-wave propagation through the sample, any increase in α leads to a faster arrival of the detected temperature change at the sample back surface, and a compression of the impulse response. The narrowing of the impulse response profile with decreasing temperature also leads to an increase in the amplitude of the signal, which is the reason for the

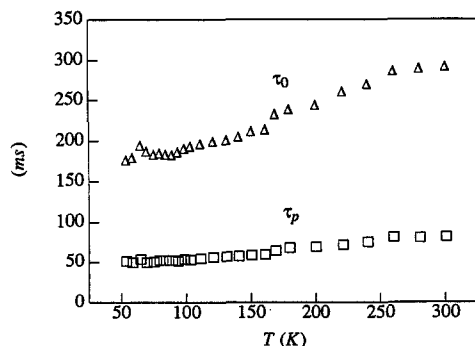


Fig. 2. Behavior of the time delay variables τ_p and τ_0 for YBCO in the temperature range 50–300 K.

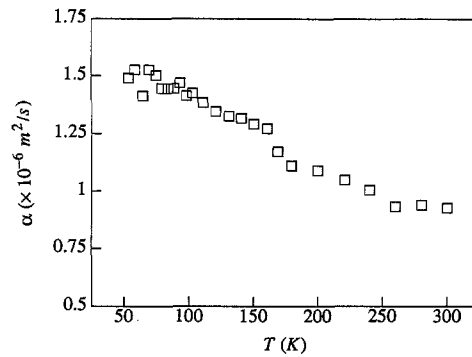


Fig. 3. Temperature dependence of the thermal diffusivity for YBCO

normalization applied in Fig. 1. This decrease in τ_p and τ_0 at lower temperatures is thus indicative of a concomitant increase in the thermal diffusivity. The τ_0 curve, furthermore, exhibits a discontinuous jump near T_c ; the jump is also present in the τ_p curve, albeit at a lower resolution because of the slower rate of change of this parameter. Note that τ_p is inversely proportional to α , and thus proportional to C/κ . Although both κ and C change around the transition temperature, the thermal conductivity is continuous [10, 11], and so the fractional jump $\Delta\tau_p/\tau_p$ will be approximately equal to the fractional change in specific heat $\Delta C/C$. From this relation we may estimate the specific heat jump to be 4% of the total specific heat.

The temperature dependence of the thermal diffusivity is shown in Fig. 3, calculated from (7). The curve exhibits two interesting points: a dip near the transition from the normal to the superconducting state; and a local minimum just below the transition temperature. As we shall see later, this dip correlates with a local maximum of the thermal conductivity at this temperature. The α vs T profile is in good agreement with data using photoacoustics and laser flash measurements [13] as well as with our previous chirped laser measurements of the thermal diffusivity of YBCO [20–22].

Figure 4 shows the temperature dependence of the thermal conductivity, calculated from (6). While κ decreases as the temperature is lowered, there is a rapid increase below T_c and then a maximum at a temperature significantly lower than T_c . This behavior has also been observed elsewhere [10–12] and has been related to the suppression of the phonon-carrier scattering mechanism.

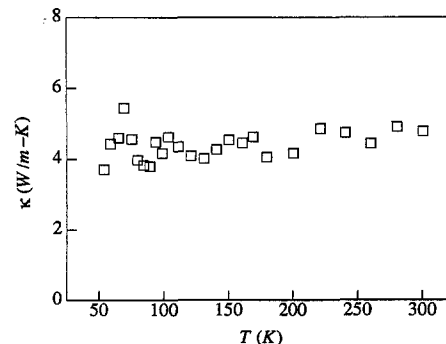


Fig. 4. Temperature dependence of the thermal conductivity YBCO

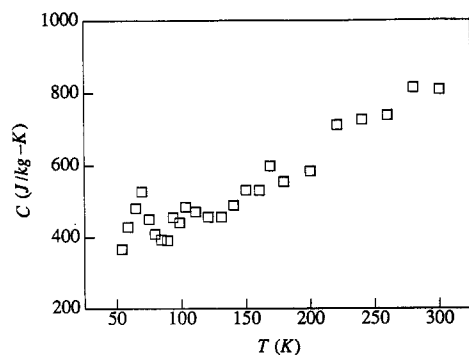
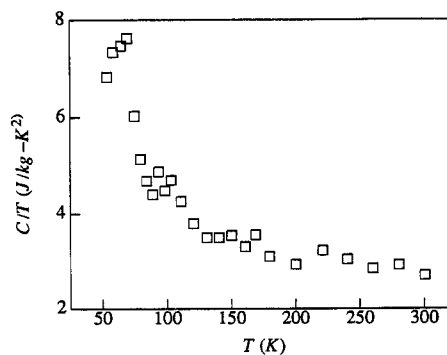


Fig. 5. Temperature dependence of the specific heat for YBCO


 Fig. 6. Temperature dependence of C/T for YBCO

The measured thermal conductivity may be written as $\kappa = \kappa_c + \kappa_p$, where κ_c is the contribution due to carriers and κ_p the phonon contribution. Previous studies [10] have made estimates of the upper limit of the carrier thermal conductivity at T_c to be $\kappa_c = 4 \times 10^{-2} \text{ W/m} \cdot \text{K}$. This value accounts for less than 1% of our thermal conductivity at this temperature, implying that nearly all the heat is transported by lattice vibrations. This result is consistent with the conclusion of other workers.

In Fig. 5 we show the behavior of the specific heat and in Fig. 6 the temperature dependence of C/T , as calculated from (8). Although the density of YBCO has been reported to exhibit an anomalous change [33, 34] at T_c , the change is small, and so we have approximated $\rho(T)$ by a slowly varying function, which is a linear fit of the reported $\rho(T)$ neglecting the region around T_c . The resulting difference in C or C/T from otherwise using $\rho(T) = \rho(300 \text{ K}) = 6.383 \text{ g/cm}^3$, the density at room temperature determined crystallographically, is negligible.

Table 1 lists some comparisons between the thermal parameters of YBCO as measured by this work and as previously reported [10, 11, 13, 22, 26, 27, 35–37]. There is a spread in the reported values for α , κ , and C , however, which can vary by as much as one order of magnitude [38], depending on the processing conditions for the sample. Considering this spread, our measurements at particular temperatures correspond quite favorably with results on similar samples. This observation, in addition to the fact that our measurements exhibit the correct

qualitative behavior of α , κ , and C for YBCO over the entire temperature range 50–300 K, highlight the potential of our technique in the simultaneous measurement of these thermal parameters.

We should point out that the time-domain photopyroelectric technique presented here is complementary to the frequency-domain photopyroelectric method for simultaneous determination of thermal diffusivity, thermal conductivity and specific heat [27], which has also been applied to the study of superconductors over a wide range of temperatures. Taking into account the spread in thermal parameters for YBCO samples produced under different conditions, both techniques produce comparable results. The frequency-domain technique, however, requires a separate reference experiment in order to obtain absolute values for α , κ , and C ; the time-domain technique is self-calibrating and readily yields these values. On the other hand, while the frequency-domain approach allows continuous measurement during the cooling or heating cycle, the time-domain technique requires point-by-point measurements at discrete temperatures, with a dwell time on the order of at least one chirp duration; this is the reason for the higher temperature resolution for the frequency-domain technique. This disadvantage may be offset by instrumental modifications allowing for a greater degree of control of the sample temperature than was possible in our set-up. In general, photothermal techniques for the simultaneous measurement of two or more thermal parameters cur-

Table 1. Summary of measurements for thermal parameters of YBCO from the literature and as measured by FM-TDPS

$\alpha (T_c)$ [cm ² /s]	$\alpha (300 \text{ K})$ [cm ² /s]	$\kappa (T_c)$ [W/m · K]	$\kappa (300 \text{ K})$ [W/m · K]	$\Delta C/C$	Ref.
–	–	5.00	5.00	–	[10]
–	–	3.50	4.75	–	[11]
0.0130	0.0070	–	–	0.050	[13]
0.0230	0.0100	–	–	0.060	[22]
0.0225	0.0120	–	–	0.060	[22]
0.0375	–	2.75	–	–	[26]
0.0525	–	5.40	–	0.025	[27]
–	0.0710	–	–	–	[35]
–	0.0458	–	–	–	[35]
–	–	3.00	2.20	–	[36]
–	–	–	–	0.050	[37]
0.0140	0.0090	4.00	4.75	0.040	This work

rently lack the precision of measurements via separate experiments [6–12]; this is because of the derivative nature of one or more parameters in the simultaneous approach. While more sensitive instrumentation and analysis is expected to increase the precision of these measurements in the future, both impulse-response and frequency-response photopyroelectric methods in their present forms are directly applicable for obtaining measurements over a wide temperature range, to identify ranges over which more precise techniques can be applied.

4. Conclusions

In summary, we have shown that the technique of frequency-modulated time-delay photopyroelectric spectrometry, which consists of chirped laser excitation of the sample and detection of the associated impulse by a thin-film pyroelectric detector, can be used to simultaneously measure the temperature dependence of the thermal diffusivity, thermal conductivity and the specific heat of a sample. No calibration is required for the measurements, and absolute values for these thermal parameters may be obtained without having to employ a reference sample. We have applied the method to the high- T_c superconductor $\text{YBa}_2\text{Cu}_3\text{O}_{7-x}$ over the temperature range 50–300 K, obtaining values in good agreement with reported measurements of α , κ , and C , which previously required separate experiments for determination.

Acknowledgements. This work was supported by the Ontario Laser and Lightwave Research Centre (OLLRC). We also thank Dr. Hans Coufal of the IBM Almaden Research Center, for providing the samples used in this work.

References

1. A. Mandelis: *Chem. Phys. Lett.* **108**, 388 (1984)
2. H. Coufal: *Appl. Phys. Lett.* **44**, 59 (1984)
3. H. Coufal, R. Grygier, D. Home, J. Fromm: *J. Vac. Sci. Technol. A* **5**, 2875 (1987)
4. H. Coufal, R. Grygier: *J. Opt. Soc. Am. B* **6**, 2013 (1989)
5. H. Coufal, A. Mandelis: *Ferroelectrics* (1991) in press
6. S.J. Collocott, G.K. White, S.X. Dou, R.K. Williams: *Phys. Rev. B* **36**, 5684 (1987)
7. S.E. Inderhees, M.B. Salamon, N. Goldenfeld, J.P. Rice, B.G. Pazol, D.M. Ginsberg, J.Z. Liu, G.W. Crabtree: *Phys. Rev. Lett.* **60**, 1178 (1988)
8. S.E. Inderhees, M.B. Salamon, T.A. Friedmann, D.M. Ginsberg: *Phys. Rev. B* **36**, 2401 (1987)
9. M.V. Nevitt, G.W. Crabtree, T.E. Klippert: *Phys. Rev. B* **36**, 2398 (1987)
10. D.T. Morelli, J. Heremans, D.E. Swets: *Phys. Rev. B* **36**, 3917 (1987)
11. C. Uher, A.B. Kaiser: *Phys. Rev. B* **36**, 3917 (1987)
12. J.J. Freeman, T.A. Friedmann, D.M. Ginsberg, J. Chen, A. Zangvil: *Phys. Rev. B* **36**, 8786 (1987)
13. L. Gomes, M.M.F. Vieira, S.L. Baldochi, N.B. Lima, M.A. Novak, N.D. Vieira, Jr., S.P. Morato, A.J.P. Braga, C.L. Cesar, A.F.S. Penna, J. Mendes Filho: *J. Appl. Phys.* **63**, 5044 (1988)
14. Y.S. Song, H.K. Lee, N.S. Chung: *J. Appl. Phys.* **65**, 2568 (1989)
15. Y.S. Song, N.S. Chung: *J. Appl. Phys.* **67**, 935 (1990)
16. M. Marinelli, U. Zammit, F. Scudieri, S. Martellucci, J. Quartieri: *Nuovo Cimento* **9**, 557 (1987)
17. M. Marinelli, U. Zammit, F. Scudieri, S. Martellucci: *Nuovo Cimento* **9**, 855 (1987)
18. C. Glorieux, E. Scoubs, J. Thoen: *Mater. Sci. Eng. A* **122**, 87 (1989)
19. I.A. Vitkin, S.B. Peralta, A. Mandelis, W. Sadowski, E. Walker: *Meas. Sci. Technol.* **1** (1990) 184
20. S.B. Peralta, I.A. Vitkin, A. Mandelis, W. Sadowski, E. Walker: In *Photoacoustic and Photothermal Phenomena II*, ed. by J.C. Murphy, J.W. Maclachlan Spicer, L.C. Aamodt, B.S.H. Royce, Springer Ser. Opt. Sci. Vol. 62 (Springer, Berlin, Heidelberg 1990) pp. 211–213
21. S.B. Peralta: *Bull. Am. Phys. Soc.* **35**, 464 (1990)
22. S.B. Peralta, Z.H. Chen, A. Mandelis: *Ferroelectrics* (1991) in press
23. A. Mandelis, L.M.L. Borm, J. Tiessinga: *Rev. Sci. Instrum.* **57**, 622 (1986)
24. A. Mandelis, L.M.L. Borm, J. Tiessinga: *Rev. Sci. Instrum.* **57**, 630 (1986)
25. J.F. Power, A. Mandelis: *Rev. Sci. Instrum.* **58**, 2024 (1987)
26. F. Murtas, M.G. Mecozzi, M. Marinelli, U. Zammit, R. Pizzoferrato, F. Scudieri, S. Martellucci, M. Marinelli: In *Photoacoustic and Photothermal Phenomena II*, ed. by J.C. Murphy, J.W. Maclachlan Spicer, L.C. Aamodt, B.S.H. Royce, Springer Ser. Opt. Sci. Vol. 62 (Springer, Berlin, Heidelberg 1990) pp. 208–210
27. M. Marinelli, F. Murtas, M.G. Mecozzi, U. Zammit, R. Pizzoferrato, F. Scudieri, S. Martellucci, M. Marinelli: *Appl. Phys. A* **51**, 387 (1990)
28. Y.S. Touloukian, R.W. Powel, C.Y. Ho, M.C. Nicolaou: In *Thermal Diffusivity*, ed. by Y.S. Touloukian, C.Y. Ho (Plenum, New York 1973) Vol. 10
29. W.R. Donaldson, A.M. Kadin, P.H. Ballentine, R. Sobolewski: *Appl. Phys. Lett.* **54**, 2470 (1989)
30. KYNAR™ Piezo Film Technical Manual, Pennwalt Corp., King of Prussia, PA, 1983
31. I.A. Vitkin: M. Sc. Thesis, University of Toronto
32. M. Marinelli, F. Mercuri, U. Zammit, R. Pizzoferrato: *Appl. Phys. A* **52** (1991) in press
33. H. Yusheng, C. Liying, X. Jiong, L. Zhihu, L. Sihan: *J. Phys.: Condensed Matter* **1**, 1055 (1989)
34. R. Srinivasan, K.S. Girirajan, V. Ganesan, V. Radhakrishnan, G.V.S. Rao: *Phys. Rev. B* **38**, 889 (1988)
35. X. Zhang, C. Gan, Z. Xu, S. Zhang, H. Zhang: In *Photoacoustic and Photothermal Phenomena II*, ed. by J.C. Murphy, J.W. Maclachlan Spicer, L.C. Aamodt, B.S.H. Royce, Springer Ser. Opt. Sci. Vol. 62 (Springer, Berlin, Heidelberg 1990) pp. 205–207
36. V. Bayot, F. Delannay, C. Dewitte, J.-P. Erauw, X. Gonze, J.-P. Issi, A. Jonas, M. Kinany-Alaoui, M. Lambrecht, J.-P. Michenaud, J.-P. Minet, L. Piraux: *Solid State Commun.* **63**, 983 (1987)
37. M. Muller, R. Oslander, A. Gold, P. Korpiun: In *Photoacoustic and Photothermal Phenomena II*, ed. by J.C. Murphy, J.W. Maclachlan Spicer, L.C. Aamodt, B.S.H. Royce, Springer Ser. Opt. Sci. Vol. 62 (Springer, Berlin, Heidelberg 1990) pp. 198–201
38. H.E. Fischer, S.K. Watson, D.G. Cahill: *Comments Cond. Matt. Phys.* **14**, 65 (1988)